ISAR imaging Based on the Empirical Mode Decomposition Time-Frequency Representation

Orian Couderc, Jean-Christophe Cexus, Fabrice Comblet, Abdelmalek Toumi, Ali Khenchaf

▶ **To cite this version:**

Orian Couderc, Jean-Christophe Cexus, Fabrice Comblet, Abdelmalek Toumi, Ali Khenchaf. ISAR imaging Based on the Empirical Mode Decomposition Time-Frequency Representation. International Radar Symposium 2016 (IRS2016), May 2016, Cracovie, Poland. hal-01326380

HAL Id: hal-01326380

https://ensta-bretagne.hal.science/hal-01326380

Submitted on 3 Jun 2016

HAL is a multi-disciplinary open access archive for the deposit and dissemination of scientific research documents, whether they are published or not. The documents may come from teaching and research institutions in France or abroad, or from public or private research centers.

L'archive ouverte pluridisciplinaire **HAL**, est destinée au dépôt et à la diffusion de documents scientifiques de niveau recherche, publiés ou non, émanant des établissements d'enseignement et de recherche français ou étrangers, des laboratoires publics ou privés.

ISAR imaging Based on the Empirical Mode Decomposition Time-Frequency Representation

Orian Couderc, Jean-Christophe Cexus, Fabrice Comblet, Abdelmalek Toumi, Ali Khenchaf
ENSTA Bretagne - Lab-STICC, UMR CNRS 6285
2, rue François Verny, 29806 Brest Cedex 9, France.
Email: orian.couderc@ensta-bretagne.org
{cexusje,comblefa,toumiab,khencha}@ensta-bretagne.fr

***Abstract*—This work proposes an adaptation of the Empirical Mode Decomposition Time-Frequency Distribution (EMD-TFD) to non-analytic complex-valued signals. Then, the modified version of EMD-TFD is used in the formation of Inverse Synthetic Aperture Radar (ISAR) image. This new method, referred to as NSBEMD-TFD, is obtained by extending the Non uniformly Sampled Bivariate Empirical Mode Decomposition (NSBEMD) to design a filter in the ambiguity domain and to clean the Time-Frequency Distribution (TFD) of signal. The effectiveness of the proposed scheme of ISAR formation is illustrated on synthetic and real signals. The results of our proposed methods are compared to other Time-Frequency Representation (TFR) such as Spectrogram, Wigner-Ville Distribution (WVD), Smoothed Pseudo Wigner-Ville Distribution (SPWVD) or others methods based on EMD.**

***Index Terms*—Inverse Synthetic Aperture Radar, Image formation, Time-Frequency Representation, Empirical Mode Decomposition.**

I. Introduction

In the ISAR imagery, a classic approach is to consider the data as stationary signals. Then, the image is built using Fourier Transforms (FT) [1]. However the ISAR technique is characterised by the movement of the target that induced the apparition of Doppler frequency making signals non-stationary [2]. Thus, the image construction goes through a chain composed of FT and movement estimation to compensate the non-stationary nature of the ISAR data [1]. Due to this nature, time-frequency methods have been introduced in the radar imaging field [3], [4]. By generating a TFR from each Doppler profile, a cube of data is build. It constitutes the evolution through time of the ISAR images. In [3], TFR like the Spectrogram or the WVD are used. Others have tried less conventional TFR like a S-method [5] or a harmonic wavelet decomposition [6]. In time-frequency methods, the WVD has a number of desirable properties that make it a good indicator of how the energy of the signal can be viewed. Nevertheless, drawbacks of the WVD are the presence of interferences for multicomponent signals. These cross-terms make the transform space of WVD difficult to visually interpret [7]. This statement leads to the attempt to reduce them and to keep a good resolution. In this objective, the SPWVD sets two filters, one to filter in the time domain and another to filter in the frequency domain. On one side of our approach, we will use some of those TFRs after decomposing the signal. A decomposition is done to reduce cross-term interferences. The Empirical Mode Decomposition (EMD) is a process put in place in the late 90's which decomposes iteratively a real signal into monocomponent signals [8]. Those signals extracted from high frequency to low frequency are called Intrinsic Mode Functions (IMF) and the last signal extracted which depicts the trend of the signal is the residu. These IMF are defined with the following properties [8]: all the local maxima must be positive, all the local minima must be negative and the sum of the upper hull and the lower hull built by interpolating the local extrema should be null. Hence, the signal x is decomposed:

$$x(t) = \sum_{i=1}^{N} IMF_i(t) + r(t) \ , \tag{1}$$

where r is the residual signal and IMF_i is the ith IMF extracted. The sifting algorithm (process to extract IMFs) shows some issues [9]. The identification of local extrema is crucial to the good construction of the hulls so as the interpolation of the extrema. In general, a cubic spline interpolation is used. Another matter is about the signal edges and the interpolation of the extrema at these locations. Some solutions are provided to these issues like mirroring the signal or weighting it with a smooth window in order to avoid divergences at the hulls edges. The EMD has also the property to act as a filter bank on the signal [10].

With the complex non-analytic ISAR data, we will use the complex versions of the EMD. There are two main versions: CEMD (Complex Empirical Mode Decomposition) and BEMD (Bivariate Empirical Mode Decomposition).
CEMD [11] decomposes the original signal by separating the positive from the negative components of the signal spectrum. These two analytic sub-signals are made real in order to be able to apply the original EMD. With two sets of IMF, one corresponding to the positive frequency components of the signal and the other one to the negative. The IMF of the signal are the analytic form of each IMF. This method have been applied on radar [12] and ISAR imagery [13].
BEMD [14] is closer to the EMD process than the CEMD. By looking at the signal as two components making it rotating through time it defines a signal hull as a surface

embracing the shape of the signal. The local mean is defined as the centre of each section of this surface. Like the original EMD the subtraction of the local mean to the signal gives the next IMF to treat. In practice, to compute the signal hull is the result of interpolating maxima from projections of the signal along different directions. This approach is suitable to Doppler profiles generated with a modeled target by scatterers. Doppler profiles are then composed of several time-frequency chirps (*i.e.* rotating signals) due to the target's motion.

A variation of the BEMD, NSBEMD (Non uniformly Sampled BEMD), have been proposed in [15]. Instead of taking a uniform distribution of directions in the bivariate plane, we can look at the main direction of the signal in the complex plane and then sample the directions on the ellipse defined with this main direction and the power imbalance of the two signal components (real part and imaginary part). In [14], it is recommended to use no more than 16 directions to compute a BEMD. This is the same number of directions used for the BEMD and the NSBEMD in the following approaches.

The paper is organized as follows. Section II gives an overview of ISAR formation with TFR and the methods based on complex versions of EMD. Some simulations and comments are proposed in section III. Finally, the last section gives some conclusions and remarks.

II. ISAR Imaging using Time-Frequency Analysis

A. Principle of Radar Imaging Based on Time-Frequency

To compute a focused ISAR image of maneuvering targets, a Time-Frequency Transforms is desirable. Figure 1 shows the radar imaging system based on the TFR [1].

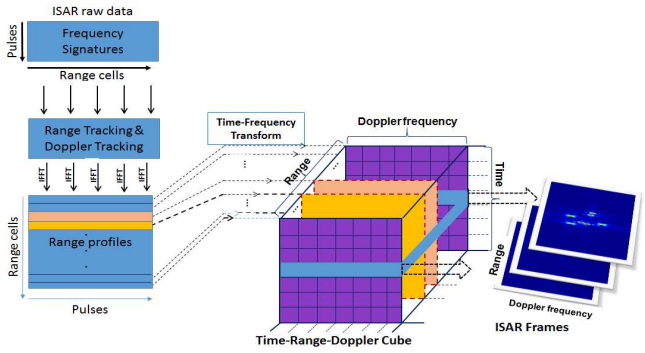

Fig. 1. Flowchart of ISAR image formation based on joint TFR.

As in [13], the combination of CEMD and TFR can be applied on ISAR image formation. On each Doppler profile, a complex EMD is performed. Summing the TFRs from IMFs generates the TFR of the profile as shown in figure 2.

In fact, in these approaches, complex EMD methods (*e.g.* CEMD, BEMD, NSBEMD) are used in conjunction with TFR (*e.g.* Spectrogram, WVD, SPWVD...). The output is a Time-Frequency representation which could be approximated as:

$$\Upsilon^{x}_{EMD-TFR}[t,f] \simeq \sum_{i=1}^{N} TFR[IMF_i(t)] \ . \qquad (2)$$

However the main problem with such methods is that the EMD does not always accurately decompose multicomponents non-stationary signals.

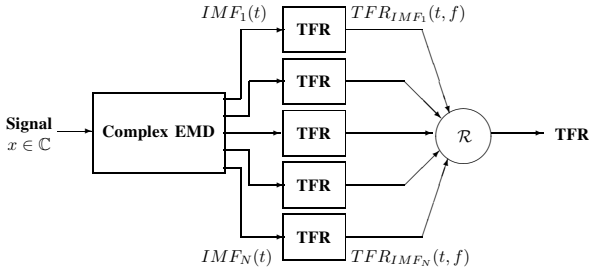

Fig. 2. Flowchart of TFR using complex versions of EMD based on [13].

B. Principle of Modified Version of EMD-TFD

An interesting time-frequency method called EMD-TFD is developed in [16], [17]. The approach rests on filtering the WVD interferences through the ambiguity function $A_x(\nu,\tau)$ of x is defined as [7]:

$$\iint_{-\infty}^{+\infty} A_x(\nu,\tau) e^{-2i\pi(\nu t+\tau f)}\, d\nu\, d\tau = WV_x(t,f) \ , \qquad (3)$$

where $WV_x(t,f)$ denotes the WVD of x, $A_x(\nu,\tau)$ is the ambiguity function, τ is time-lag and ν is Doppler variable.

To threshold the ambiguity function, two criteria are proposed:

- **Energy criterion [16]**: The user sets the energy ratio t_h between the filtered ambiguity function of the IMF and the ambiguity function of the signal (equation (4)). This ratio is reached by finding the good threshold r to apply on the ambiguity function of the considered IMF $A_{IMF_i}(\nu,\tau)$ (equation (5)). If this ratio r cannot be reached for any r then the IMF is left out.

$$\frac{\iint_{-\infty}^{+\infty} G_{IMF_i}(\nu,\tau) A_{IMF_i}(\nu,\tau)\, d\nu\, d\tau}{\iint_{-\infty}^{+\infty} A_x(\nu,\tau)\, d\nu\, d\tau} \geq t_h \ , \qquad (4)$$

$$G_{IMF_i}(\nu,\tau) = \begin{cases} 1 & if \ \ |A_{IMF_i}(\nu,\tau)| \geq r \\ 0 & otherwise \end{cases} \ . \qquad (5)$$

- **Criterion on the maximum [17]**: The user defines directly the threshold r used in the equation (5). This threshold is used for every IMF.

The EMD-TFD uses the EMD to design a filter and then to clean in the ambiguity domain the analytic signal. After computing the ambiguity function for each IMF, they are thresholded using an energy criterion or a criterion on the maximal value of the function. Those thresholded functions

are combined by meaning them or by applying a logical OR. This combination provides a coarse filter that will be smoothed through a 2D window before cleaning the ambiguity function of the signal. The scheme (figure 3) summaries this process. So, the EMD-TFD is then defined as [17]:

$$\Upsilon_{EMD-TFD}(t,f) = \iint_{-\infty}^{+\infty} G(\nu,\tau) A_x(\nu,\tau) e^{-2i\pi(\nu t+\tau f)} \mathrm{d}\nu \mathrm{d}\tau \tag{6}$$

where $G(\nu,\tau) = \mathcal{R}_{i=1}^{n}[G_{IMF_i}(\nu,\tau)]$.

C. ISAR Imaging Algorithm Based on NSBEMD-TFD

The adaptation of the EMD-TFD to complex signal is done by using the NSBEMD instead of the original EMD (figure 3).

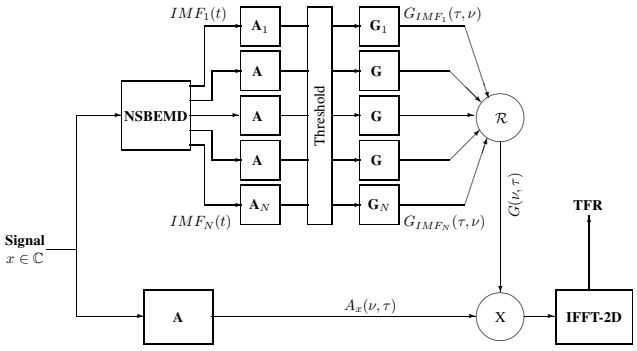

Fig. 3. Flowchart of the NSBEMD-TFD based on [17].

***A** box is the transformation from a signal to its ambiguity function (3), **NSBEMD** box provides IMFs of the input signal, **G** boxes are the operations done to smooth the thresholded ambiguity functions, $\mathcal{R}$ box represents the operation of filters combination and **X** operand is the filter operation in the ambiguity domain.*

In order to determine the value of the threshold and the length of the window used to smooth the thresholded ambiguity function, the intensive simulations have been computed on a known signal. In general, thresholding the modulus of the ambiguity function shows nicer performance in keeping the sharpness of the representation and removing interferences. Good results can be obtained with a threshold set between 0.2 and 0.5 and a ratio between the length of the Hanning window and the signal around 0.06. The second way to create filters based on a energy criterion is left out due to its poor performance. Likewise these parameters used to define the method can be determined for the creation of ISAR images.

III. Results

A. Simulated Data

We tested our approach on the simulated MIG25 dataset described in [1]. Figure 4(a) shows the simulated target model, and it consists of 120 point scatterers of equal reflectivity. The raw data contains 512 recurrences of 64 range bins. All simulations are first put on a logarithmic scale and then normalised. The Spectrogram applied to create ISAR image uses a Hanning window with the same length as the Doppler profil. A Hanning windows of one tenth (respectively a quarter) of the Doppler signal length is used to filter in time (respectively in frequency) the WVD in the SPWVD method. For the NSBEMD-TFD based on equation (6), the threshold is set at 0.35 and the Hanning window is one-sixteenth of the Doppler profile length.

Figure 4(c) shows the ISAR image using WVD. The WVD shows the blurred effects. It is explainable by the intense interference in the image and then the low contrast between the background and the target representation. Figures 4(b) and 4(d) show reasonable agreement with the ideal point scatterers using Spectrogram and SPWVD, respectively. From these results, SPWVD has better performance of resolution than the Spectrogram or WVD. On the results obtained from NSBEMD-TFD (Figure 4(e)), we can observe that the components are well estimated, reduced cross-term interference with a good resolution and shows a nice dynamic.

Figures 5, 6 and 7 show the results of combining the complex EMDs and TFRs based on equation (2): CEMD-TFR, BEMD-TFR and NSBEMD-TFR, respectively. For these TFRs are Spectrogram, WVD and SPWVD, respectively. Comparing the $\{$CEMD,BEMD,NSBEMD$\}$-WVD against the WVD, we see that the components are well estimated and reduced cross-term interference. The NSBEMD-SPWVD (figure 7(c)) shows a very interesting performance in the image dynamic, a good resolution and, in reducing interferences but the smoothing effect is too harsh. So, the scattering points have a nice resolution but the intensity of point scatterers is much less than Figure 4(e). Large number of the methods based on complex EMDs provide interesting performance when the time-frequency energy is presented by the concentration and resolution of TFR along the individual component of the multi-components (non-stationary) signals.

B. Real Data

We put under trial the time frequency methods and the quality criteria by acquiring data with the anechoic chamber of ENSTA Bretagne. In order to be close to the target model, we build a target composed of three metal balls. They are placed in a isosceles triangle configuration. The height of this triangle is 60cm and the length of the base is 33cm. The diameter of each ball is 4.5cm. An optical picture of the target is shown in Figure 4. This target is rotating from $[-30^o, 30^o]$ with an angular step of 0.4^o. We use a step-frequency radar with a central frequency of 10GHz, a bandwidth of 8GHz and 101 points of measures (*i.e.* a frequency step of 78MHz). This set up allows us to have a range resolution of 1.8cm and a cross-range resolution of 1.4cm.

The figure 8(b) shows ISAR images generated from Spectrogram, WVD, SPWVD, NSBEMD-SPWVD based on equation (2) and, NSBEMD-TFD based on equation (6), respectively. The same observations as for the simulated data

can be made. For the NSBEMD-TFD, we have a better view of the interference within each IMF effects. We can also notice that in this case the SPWVD is filtering better than on simulated data and in general, there are less interferences. This last statement can be due to the fact that we use only three balls when with simulated data 120 points are used.

IV. Conclusions

This paper presents the adaptation of a TFR using the EMD to non-analytic complex signal and its application to ISAR image formation. Those adaptations have been tested first on simulated data and then on data acquired from an anechoic chamber. The performance of the proposed method is compared with conventional TFR methods (Spectrogram, WVD, SPWVD). The most original approach employs the EMD to design a filter used in the ambiguity domain of the signal. The strength of the method relies on building a filter without preconceived considerations on its shape thanks to the EMD. The obtained results show that the proposed approach is an effective and a promising imaging method for ISAR image formation. Nevertheless, this technique is empirical, so further theoretical explanation work is needed and a large class of data are necessary to con?rm the obtained results. As future work, we plane to study the NSBEMD-TFD in noisy environment and we intend to address the general decision-making process (target identi?cation).

References

[1] V. C. Chen and M. Martorella, *Inverse Synthetic Aperture Radar Imaging - Principles, Algorithms and Applications*. SciTech Publishing, 2014.

[2] V. C. Chen, R. Lipps, and M. Bottoms, "Advanced Synthetic Aperture Radar Imaging and Feature Analysis," in *Proceedings of the International Radar Conference, 2003*, 2003, pp. 22–29.

[3] V. C. Chen and H. Ling, *Time-Frequency Transforms for Radar Imaging and Signal Analysis*. Artech House Publisher, 2002.

[4] ——, "Joint Time-Frequency Analysis for Radar Signal and Image Processing," *Signal Processing Magazine, IEEE*, vol. 16, no. 2, pp. 81–93, 1999.

[5] L. J. Stankovic, T. Thayaparan, M. Dakovic, and V. Popovic, "S-Method in Radar Imaging," in *Signal Processing Conference, 2006 14th European*, vol. 10, 2006, pp. 1–5.

[6] B. Shreyamsha Kumar, B. Prabhakar, K. Suryanarayana, V. Thilagavathi, and R. Rajagopal, "Target Identification Using Harmonic Wavelet Based ISAR Imaging," *EURASIP Journal on Applied Signal Processing*, vol. 2006, pp. 1–13, 2006.

[7] B. Boashash, *Time-Frequency Signal Analysis and Processing - A Comprehensive Reference*. Elsevier, 2003.

[8] N. E. Huang, Z. Shen, S. R. Long, M. C. Wu, and *et al.*, "The Empirical Mode Decomposition and the Hilbert spectrum for nonlinear and non-stationary time series analysis," *Proceedings of the Royal Society of London A: Mathematical, Physical and Engineering Sciences*, vol. 454, no. 1971, pp. 903–995, 1998.

[9] G. Rilling, P. Flandrin, and P. Gonçalves, "On Empirical Mode Decomposition and its Algorithms," in *Proceedings of IEEE-EURASIP Workshop on Nonlinear Signal and Image Processing NSIP-03*, June 2003, pp. 8–11.

[10] ——, "Empirical Mode Decomposition as a Filter Bank," *IEEE Signal Processing Letters*, vol. 11, no. 2, pp. 112–114, 2004.

[11] T. Tanaka and D. Mandic, "Complex Empirical Mode Decomposition," *IEEE Signal Processing Letters*, vol. 14, no. 2, pp. 101–104, 2007.

[12] B. Bjelica, T. Thayaparan, M. Dakovic, and M. Dakovic, "Complex Empirical Decomposition Method in Radar Signal Processing," in *Mediterranean Conference on Embedded Computing*, 2012.

[13] B. A. H. Ahmed, J.-C. Cexus, and A. Toumi, "ISAR Image Formation with a Combined Empirical Mode Decomposition and Time-Frequency Representation," in *Proc. EUSIPCO'15*, 2015, pp. 1366–1370.

[14] G. Rilling, P. Flandrin, P. Gonçalves, and J. Lilly, "Bivariate Empirical Mode Decomposition," *IEEE Signal Processing Letters*, vol. 14, no. 12, pp. 936–939, 2007.

[15] A. Ahrabian, N. U. Rehman, and D. Mandic, "Bivariate Empirical Mode Decomposition for Unbalanced Real-World Signals," *IEEE Signal Processing Letters*, vol. 20, no. 3, pp. 245–248, 2013.

[16] N. J. Stevenson, M. Mesbah, and B. Boashash, "A Time-Frequency Distribution based on the Empirical Mode Decomposition," in *Signal Processing and Its Applications, 2007. ISSPA 2007. 9th International Symposium on*, 2007, pp. 1–4.

[17] ——, "Multiple-View Time-Frequency Distribution based on the Empirical Mode Decomposition," *IET Signal Processing*, vol. 4, no. 4, pp. 447–456, 2010.

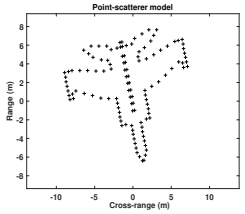

(a) Synthetic target geometry.

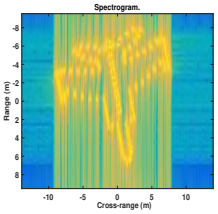

(b) Spectrogram.

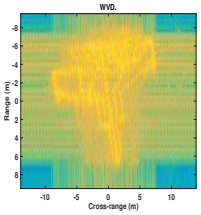

(c) WVD.

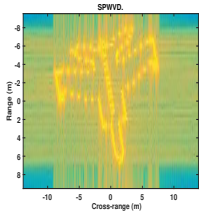

(d) SPWVD.

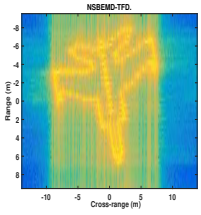

(e) NSBEMD-TFD.

Fig. 4. Comparison of ISAR image based on TFR (frame 391).

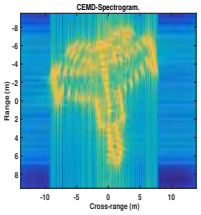

(a) CEMD-Spectrogram.

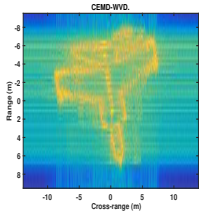

(b) CEMD-WVD.

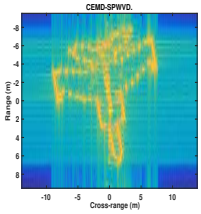

(c) CEMD-SPWVD.

Fig. 5. Comparison of **CEMD-TFR** based image (frame 391) [13].

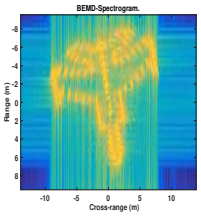

(a) BEMD-Spectrogram.

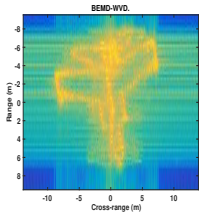

(b) BEMD-WVD.

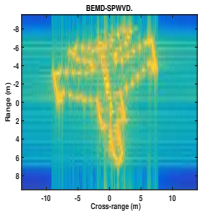

(c) BEMD-SPWVD.

Fig. 6. Comparison of **BEMD-TFR** based image (frame 391).

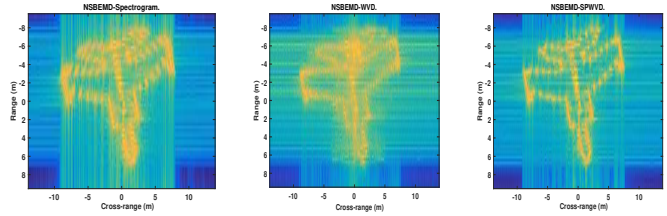

(a) NSBEMD-Spectrogram (b) NSBEMD-WVD. (c) NSBEMD-SPWVD.

Fig. 7. Comparison of **NSBEMD-TFR** based image (frame 391).

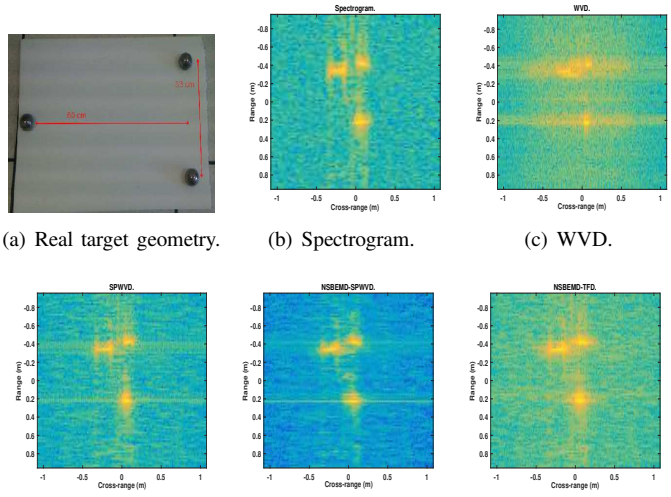

(a) Real target geometry. (b) Spectrogram. (c) WVD.

(d) SPWVD. (e) NSBEMD-SPWVD. (f) NSBEMD-TFD.

Fig. 8. Comparison of ISAR images generated with different TFR on real data (frame 36, angle$= -16^o$).